Abstract

Abstracts do not include sources, but are here for the purpose of notes.)

The physical processes that creates electrical signals in neurons are well understood, but how the signals are processed into actions and thoughts has yet to receive a scientifically robust answer (add more sources) [10]. Cell type classification is of high importance because the function of different neurons is still largely a mystery.

Contents

1 | Introduction

Introduce the topic, the problem and how the problem is being solved.

Since the conception of neuroscience the neurons function have been studied on many levels and with many perspectives, from a single neuron level to networks of neurons with chemistry, physics, medicine and psychology to name some.

2 | Theory

Each section introduces topics that are referenced frequently in the article. At the end of each section there is a background subsection. These subsections contain information about the current state of research on the topic and previous work.

2.1 The Neuron

Neurons are excitiable brain cells capable of transmitting voltage changes across its structure which again can excite other neurons. These sharp voltage changes are called action potentials and when a neuron creates an action potential it is said to "fire".

(TODO: Add picture of neuron and explain all the parts.)

(TODO: Add more, citations.)

Topic to mention: Neuron cell types, pyramidal neurons, basket neurons interneurons, what are they. The term "morphology". Intracellular also referred to as membrane potential. Subcortical. Se hemalainen p.421. for a good summary. What is transmembrane current. Impulse. Apical dendrites. Grey matter. Spines. Synapses. Quiescent neuron.

Background

The physical processes in and around neurons are well understood in comparison to the function they serve. The basic function of a neuron is to receive and send action potentials to process information. What information is transmitted and how it is processed is still being researched.

2.2 Action Potentials

Describe how actionpotentials are created.

This be a neuron yo.

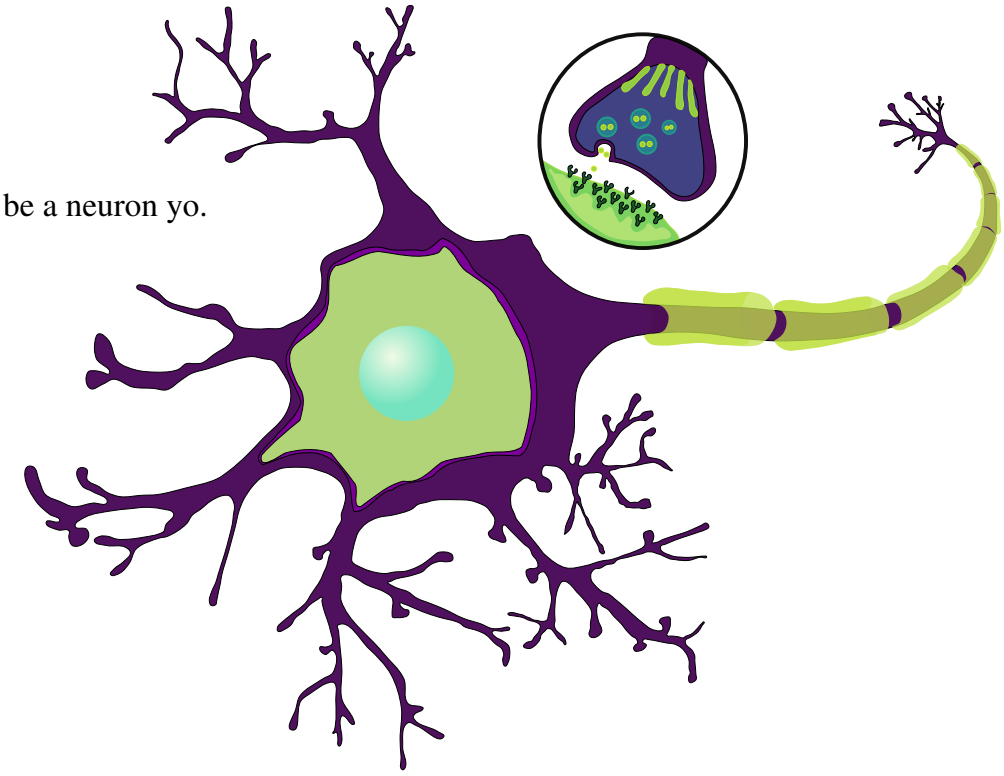

Figure 2.1: Stuff about this neuron.

Background

Write about hodking and huxley. [5]

2.3 Electrical Activity

The electrical activity of neurons are caused by different concentrations of ions in the extracelluar and intracellular medium. The cell membrane consists of a $5\,\mathrm{nm}$ lipid bilayer and is impenetrable to ions. The gradient is created by differnt ion channels and ion pumps in the cell membrane which can have selective permeability to ions. The most significant ions in this process are sodium (Na^+), potassium (K^+), calcium (Ca^{2+}), magnecium (Mg^{2+}) and chloride (Cl^-). Ion channels are divided between passive channels and active channels where the active can change the permeability under certain conditions while passive channels have a constant permeability.

There are multiple models for neurons, some of the main groups are point models and compartmental models. List many models? Multi-compartmental models can be useful to understand the processing of neurons with complex morphological structures

Background

Hodgkin & Huxley [5], Connor & Stevens [1], and Sterratt et al. [10]

The temperature is important.

2.4 Electrodes

2.5 Calculating Extracellular Potential

The extracellular potential is the electric potential generated from the transmembrane currents in the neurons. When a neuron fires this can be seen from the extracellular potential which will have a spike which is similar to the intracellular spike.

By modelling the neuron as compartments and approximating each compartment as a spherical volume current source at position $\mathbf{r_0}$, the potential at at position $\mathbf{r}$ at time t will be,

$$\mathbf{E}(\mathbf{r}, \mathbf{t}) = \frac{1}{4\pi\sigma}\frac{I_0(t)}{|\mathbf{r} - \mathbf{r_0}|} \tag{2.1}$$

$$\mathbf{E}(\mathbf{r}, \mathbf{t}) = \sum_{n=1}^{N} \frac{1}{4\pi\sigma}\frac{I_n(t)}{|\mathbf{r} - \mathbf{r_0}|} \tag{2.2}$$

Potential from compartments modelled as line sources.

$$\mathbf{E}(\mathbf{r}, \mathbf{t}) = \frac{1}{4\pi\sigma}\sum_{n=1}^{N} I_n(t)\frac{dr_n}{|\mathbf{r} - \mathbf{r_0}|} \tag{2.3}$$

$$= \frac{1}{4\pi\sigma}\sum_{n=1}^{N} I_n(t)\frac{1}{\Delta s_n}\log\left|\frac{\sqrt{h_n^2 + \rho_n^2} - h_n}{\sqrt{l_n^2 + \rho_n^2} - l_n}\right| \tag{2.4}$$

Taken from Lindén et al. [6]

This equation rests on two assumptions,

1. The permeability μ of the extracellular medium is the same as that of vacuum μ_0.
2. The quasistatic approximation which lets the time derivatives, $\partial E/\partial t$, be ignored as source terms. See appendix A.1

The extracellular potential can be calculated using Maxwell's equations and the continuity equation if the spatial distribution (morphology) of transmembrane currents and the extracellular conductivity is known.

In the quasistatic approximation, since $\nabla \times \mathbf{E} = \mathbf{0}$, the electric field can be expressed with a scalar potential.

Forward problem = calculate the potential from the current source, inverse problem is used in magnetoenchephalography (important). The amplitude of a spike in the extracellular potential is usually in the magnintude of $< 200\mu$V. The noise of electrodes vary, but can be as much as 20μV. This limits the range electrodes can record from.

The currents sum to zero, while the spike is very visible, there are many small currents in the dendrites with opposite current. ([4])

The extracellular spike width tend to increase with distance from soma because of the neuronal morphology. This article used a passive neuron model with different morphologies to

show that the spike width increases with distance to soma. The spike amplitude also decreases with distance to soma and seems to follow a power law. ([9]).

The shape of extracellular spikes are mainly depedent on the membrane currents and the morphology of the cell. Some of the effects from the morphology of the cell are increased spike width and decreased amplitude from distance to soma.

Many things here from around page 245. When the conductivity σ and the current generators are know, Maxwell's equations and the continuity equation equation can be used to calculate the electric field E and magnetic field B. (TODO: Copied text) ([4])

Background

Recording is usually done using electrodes, this makes recording the membrane potential more challenging than recording from the extracellular medium as the electrode has to be very close or inside the cell. At the time of writing, recording the membrane potential of a concious subject is nearly impossible, this makes understanding extracellular potentials vital for current research.

Early calculations was done by Rall 1962 investigating the interaction between action potentials and synapes using cylinders as the current source. (TODO: Read article, make more understandble.) Holt and Koch 1999 added comparmental models to reconstruct pyramidal neurons.

The information about the transmembrane current is usually difficult to obtain, as well as the morphology.

2.6 Neuron & LFPy

LFPy is a Python module that uses Neuron and the mentioned methods to calculate the electric field outside the neuron. [6]

Background

2.7 Cell Type Classification

Background

It was early observed that the shape of action potentials are different for individual neurons. Mountcastle et al. [8] discovered what they called regular spiking , fast spiking
[8].

2.8 Allen Cell Types Database

The Allen Brain Institute have gather individual neuron data from lateral geniculate nucleus (LGN) and primary visual cortex (V1) of young laboratory mice. The data's main categories are electrophysiology, morphology and modeling. With the morphological data the extracellular potential can be calculated given a model for the transmembrane currents.

3 | Methods

3.1 Pettersen & Einevoll (2008) Reproduction

To verify that the simulation environment can be trusted it was attempted to reproduce some results from Pettersen & Einevoll [9]. Spesifically the spike width and amplitude dependency in relation to distance from soma should be the same.

3.1.1 Simulation

Cell: The Mainen & Sejnowski [7] cell was used with a passive model, which is the same model used in Pettersen & Einevoll [9]. It is not clear in which plane the measurements was taken from so the cell was rotated using PCA (principal component analysis) on the compartment positions. This rotates the cell so most of the dendrites are along the y and x-axis.

Spike Generation: An action potental was generated using the Connor-Stevens model [1, 2] using the same parameters as Dayan & Abbott [3]. This had an amplitude of $107.6mV$ from baseline with the peak at $48.21mV$. These values are similar (TODO: how similar?) to Dayan & Abbott [3], but not with Pettersen & Einevoll [9] which had an amplitude of $83mV$ from baseline. To compensate for the difference the action potental was normalized to $83mV$ manually (fig. 3.1).

Parameters: Parameters are the same as Pettersen & Einevoll [9] and Dayan & Abbott [3] . Membrane resistance $R_m = 3 \cdot 10^4 \Omega/cm^2$, membrane capacitance $C_m = 1\mu F/cm^2$, axial resistance $R_a = 150\Omega/cm^2$, time resolution $dt = 2^{-6}ms$. The reversal potential was set to zero.

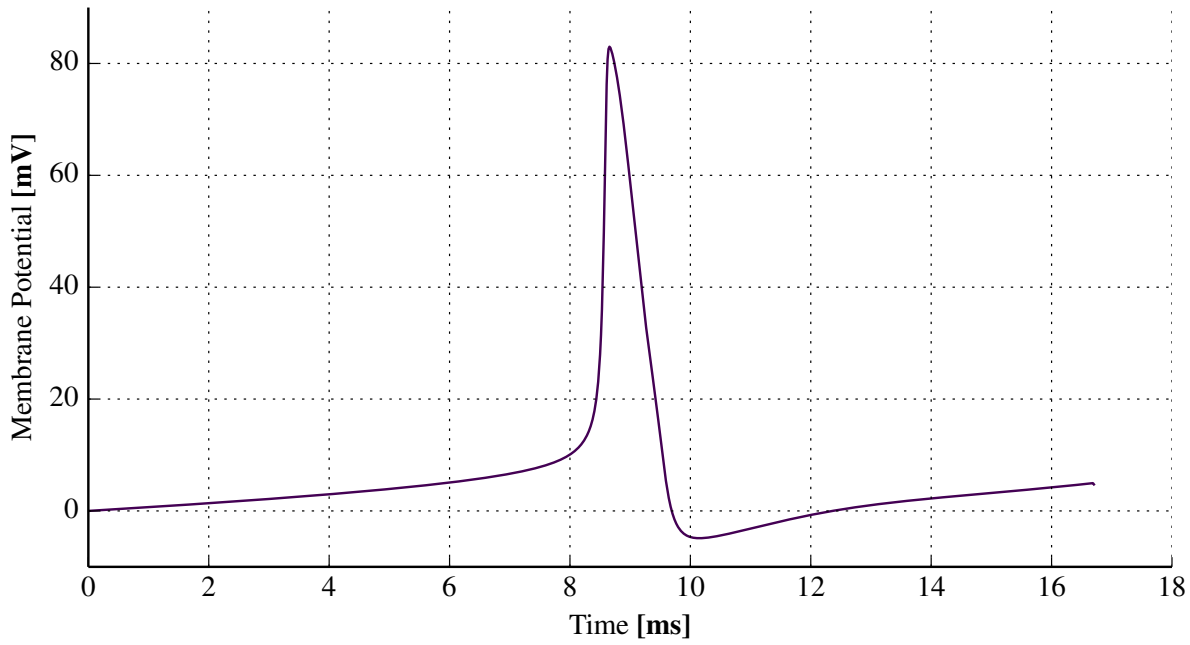

Figure 3.1: Soma membrane voltage.

The action potental was imposed in all soma sections using the "play" vector function in Neuron.

Electrode Positions: Recording sites were placed in the xz plane at 11 linearly spaced positions along 36 lines with equal angular spacing. (TODO: Show the electrode positions.)

Spike Width & Amplitude: A baseline was set as the value at the start of the signal. Amplitude was calculated as the difference between maximum absolute value and the baseline. The spike width was calculated at half width at maximum amplitude.

Spike width was recorded at $0.5625ms$ for $dt = 2 \cdot 10^{-5}$, similar to $0.55ms$ from Pettersen & Einevoll [9]. When increasing the resolution to $dt = 2 \cdot 10^{-6}ms$ the spike width rose to $0.625ms$.

3.1.2 Results

The action potental that was used in Pettersen & Einevoll [9] is similar to the one used here. The amplitude of the fourier transform is displayed in fig. 3.2 , which is in close resemblance to the standard action potential in Fig. 3 in the paper.

The spike width increases with the distance from soma as seen in fig. 3.3 . These results are lower than the widths reported in Pettersen & Einevoll [9]. (Use more time on editing the Connor-Stevens model to come closer to an max.amplitude on 20mV?).

Sudden changes in spike width was experienced with increased distance from soma. Above $200\mu V$ the spikes shapes are not well defined. This was also reported in Pettersen & Einevoll [9].

Pettersen & Einevoll [9] reports a spike amplitude above $150\mu V$ at $20\mu m$, this does not

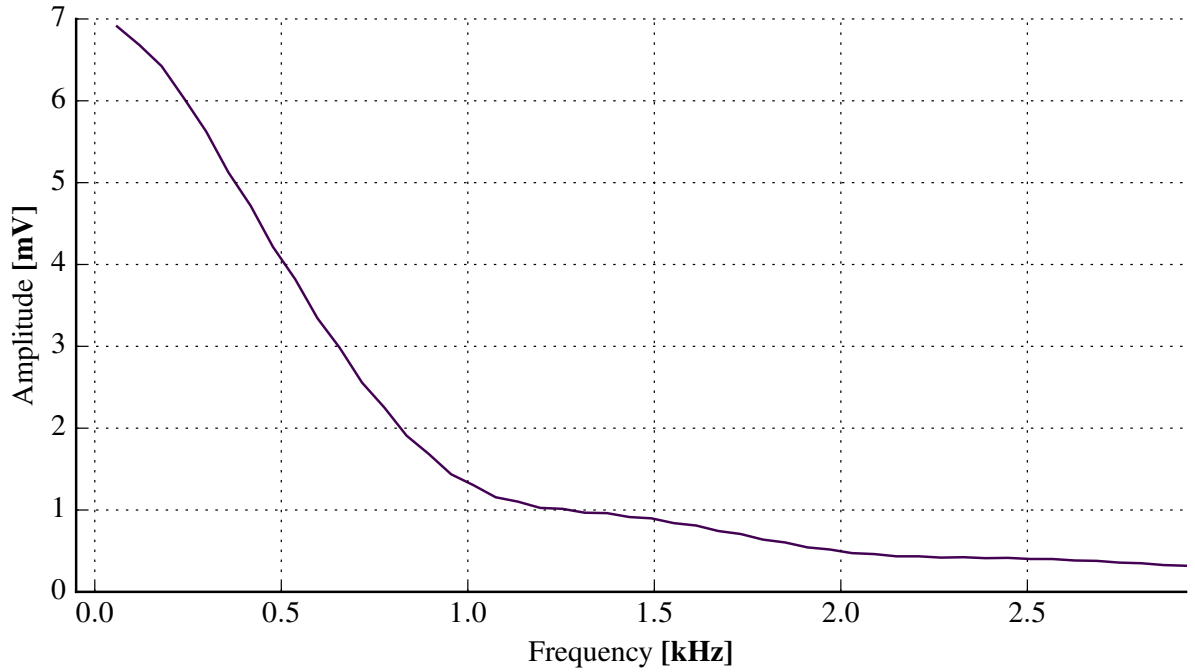

Figure 3.2: Frequency specter of simulated somatic membrane potential.

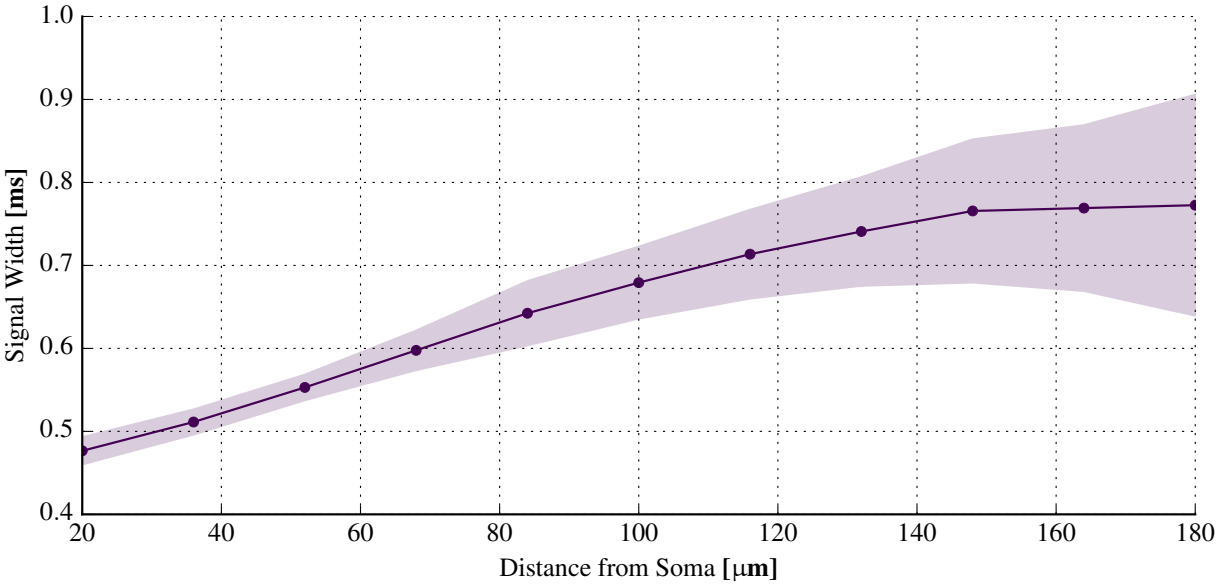

Figure 3.3: Spike width over distance. Mean +/- 1 std.

match current findings. fig. 3.4 shows spike amplitude with logarithmic axes. (TODO: Is numbers on the power law decays necessaryy?) Although the data does not match Pettersen & Einevoll [9], it is comparable with what is expected in the near and far limit field of a ball and stick neuron. In the near field the the expectation is a $1/r$ decay and in the far field it is $1/r^2$ or $1/r^3$ depending on distance. (TODO: Clearify this, put reference back to theory chapter.)

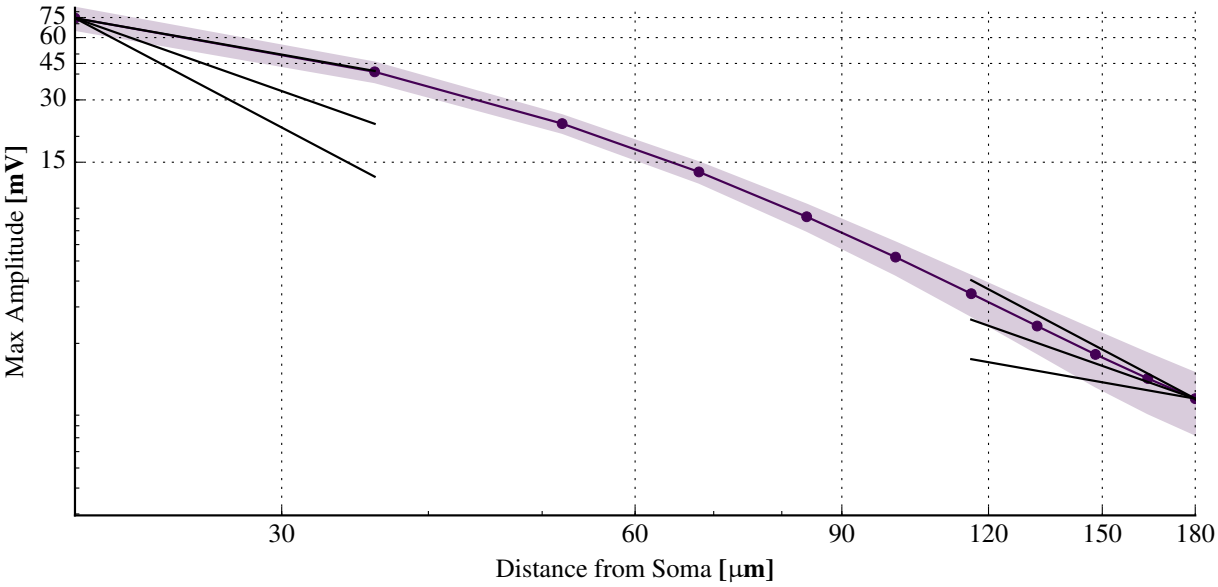

Figure 3.4: Spike amplitude over distance. Mean +/- 1 std. The power law decays $1/r$, $1/r^2$ and $1/r^3$ are shown at the leftmost and rightmost data points.

3.1.3 Discussion

3.2 Blue Brain

The Blue Brain project released XXX models based upon neurons from the hind-limb somatosensory cortex from 2-week-old Wistar Han rats. The models were used The extracellular potential was calculated using "TODO: Insert parameters here".

Use the models. Write code to capture one action potential. Bursting neurons often hav adapting action potential, what to do there.

3.3 Spike Width Measurement

Many different definitions of spike width has been used to differentiate neurons, but to date it is not clear which definition is best suited for neuron classification.

Width Type I - Peak-to-peak:

Width is measured as the time from the minimum potential to the maximum. This is the time from the polarization phase to the afterhyperpolarization phase.

Width Type II - Width at Half Amplitude:

Width is measured as the duration the spike is below half amplitude of the signal measured from the baseline at the start of the signal.

Width Type II - Width at Half Amplitude:

Width is measured as the duration the spike is below half amplitude of the signal measured from the baseline at the start of the signal.

3.4 Simulations with LFPyUtil

LFPyUtil is a python package that was created for this project with the purpose of simplifying the simulation pipeline for multiple neurons and creating and easy to use interface when developing new simulations.

In all simulations the extracellular conductivity was set to $\sigma = 0.3\,\Omega\,\mathrm{m}$ based upon data from experimental measurements.

All stimulus electrodes uses the `LFPy.StimIntElectrode` with a custom made electrode named ISyn. With the default stimulus all transmembrane currents will be summed equal the input current, using ISyn prevents this and the currents are correctly summed to 0.

The following items are python objects in LFPyUtil.

SphereRand

SphereRand places electrodes placed in uniformly distributied locations around the soma within a default radius of $50\,\mu\mathrm{m}$. Spike timing is detected by thresholding the soma membrane potential. That timing is applied to all electrodes such that all electrodes measure the same part of the simulation. If the signal has several spikes the spike index must be supplied, the default setting uses the first spike.

3.5 Allen Brain Institute

4 | Results

In figure ?? the spike width from interneurons and pyramidal neurons have been plottet seperatly. Neurons in the pyramidal group are the type TTPC1 and TTPC2 The groups suggests that interneuron can be seperated from pyramidal neurons depending on their spike shape.

5 | Discussion

Nothing here yet.

A | Appendix

A.1 Quasistatic Approximation in Neural Tissue

A quasistatic approximation implies that the equations have a form that does not include time derivatives (static). Some quantaties can be allowed to vary over time, but slowly. Here we show that the quasistatic approximation is a valid assumption in neural tissue. First start with Maxwell's equations.

$$\begin{aligned} \nabla \cdot \mathbf{E} &= p/e \\ \nabla \times \mathbf{E} &= -\partial \mathbf{B}/\partial \mathbf{t} \end{aligned} \tag{A.1}$$

$$\begin{aligned} \nabla \cdot \mathbf{B} &= 0 \\ \nabla \times \mathbf{B} &= \mu_0(\mathbf{J} + \epsilon_0 \partial \mathbf{E}/\partial t) \end{aligned} \tag{A.2}$$

In a passive nonmagnetic medium, **J** is the sum of ohmic volume current and the polarization current

$$\mathbf{J} = \sigma \mathbf{E} + \partial \mathbf{P}/\partial t \tag{A.3}$$

where $\mathbf{P} = (\epsilon - \epsilon_0)\mathbf{E}$ is the polarization and ϵ is the permitivity of the material.In neuromagnetism, we generally deal with frequencies that are below 100 Hz. Cellular electrical phenomena contain mostly frequencies below 1kHz. Let σ and ϵ be uniform and let us consider elctromagnetic wave at frequencty f.

$$\mathbf{E} = \mathbf{E}_0(\mathbf{r}) \exp(i 2\pi f t) \tag{A.4}$$

With eqs. (A.2) and (A.3) we get,

$$\nabla \times \mathbf{B} = \mu_0(\sigma \mathbf{E} + (\epsilon - \epsilon_0)\partial \mathbf{E}/\partial t + \epsilon_0 \partial \mathbf{E}/\partial t) \tag{A.5}$$

For the quasistatic approximation to be valid, it is necessary that the time-derivative terms be small compared to the ohmic current.

$$\left|\epsilon \mathbf{E}/\partial t\right| \ll |\sigma \mathbf{E}| \rightarrow 2\pi f \epsilon/\sigma \ll 1 \tag{A.6}$$

With $\sigma = 0.3\,\Omega^{-1}\,\mathrm{m}^{-1}$, the value of brain tissue, $\epsilon = 10^5 \cdot \epsilon_0$, and $f = 100\,\mathrm{Hz}$, we find

$$2\pi f \epsilon/\sigma = 2 \cdot 10^{-3} \ll 1 \tag{A.7}$$

In addition, $\partial \mathbf{B}/\partial t$ must be small. from eqs. (A.1) and (A.2) ,

$$\begin{aligned} \nabla \times \nabla \times \mathbf{E} &= -\frac{\partial}{\partial t}(\nabla \times \mathbf{B}) \\ &= -\mu_0 \frac{\partial}{\partial t}(\sigma \mathbf{E} + \epsilon \partial \mathbf{E}/\partial t) \\ &= -i2\pi f \mu_0 (\sigma + i2\pi f \epsilon)\mathbf{E} \end{aligned} \tag{A.8}$$

Solutions of this equation have spatial changes on the characteristic length scale

$$\lambda_c = \left|2\pi f \mu_0 \sigma (1 + i2\pi f \epsilon/\sigma)\right|^{-1/2} \approx 65\,\mathrm{m} \tag{A.9}$$

This length is much longer than the diameter of the head. This implies that the contribution of $\partial \mathbf{B}/\partial t$ to $\mathbf{E}$ is small. Theautorefor, the quaasistatic approximation appears justified. This does not mean that we should forget time-dependent phenomena altogether. For example, the capacitative current through the cell membrane is significant in determining the properties of the action potential. Nevertheless, this so-called displacement current, $\epsilon_0 \partial \mathbf{E}/\partial t$, need not be taken into account in the calculation of $\mathbf{B}$.

Copied from Hämäläinen et al. [4]

Glossary

A

active channels TODO 8

E

extracelluar Space outside the cell. 8

F

fast spiking A short durtion extracelluar spike. 10

I

intracellular Space inside the cell. Contains cytoplasm. 8

ion channels Proteins in the lipidbilayer that allows ion flow through the cell membrane. 8

ion pumps TODO 8

L

lipid bilayer TODO 8

P

passive channels TODO 8

R

regular spiking Often compared to fast spiking. 10

S

SphereRand Simulation object in LFPyUtil using cartesian uniformly random placed electrodes around the soma within a radius of $50\,\mu\mathrm{m}$. 15

Bibliography

[1] J. A. Connor & C. F. Stevens. “Prediction of repetitive firing behaviour from voltage clamp data on an isolated neurone soma.” In: *The Journal of Physiology* 213.1 (1971). 00704, pp. 31–53.

[2] J. A. Connor, D. Walter, & R. McKown. “Neural repetitive firing: modifications of the Hodgkin-Huxley axon suggested by experimental results from crustacean axons.” In: *Biophysical Journal* 18.1 (1977). 00236, pp. 81–102.

[3] Peter Dayan & Laurence F. Abbott. *Theoretical neuroscience*. Vol. 806. 03314. Cambridge, MA: MIT Press, 2001.

[4] Matti Hämäläinen et al. “Magnetoencephalography- theory, instrumentation, and applications to noninvasive studies of the working human brain.” In: *Reviews of modern Physics* 65.2 (1993). 03322, p. 413.

[5] Alan L. Hodgkin & Andrew F. Huxley. “A quantitative description of membrane current and its application to conduction and excitation in nerve.” In: *The Journal of physiology* 117.4 (1952). 16698, pp. 500–544.

[6] Henrik Lindén et al. “LFPy: a tool for biophysical simulation of extracellular potentials generated by detailed model neurons.” In: *Frontiers in neuroinformatics* 7 (2013). 00015.

[7] Zachary F. Mainen & Terrence J. Sejnowski. “Influence of dendritic structure on firing pattern in model neocortical neurons.” In: *Nature* 382.6589 (1996). 00880, pp. 363–366.

[8] Vernon B. Mountcastle et al. “Cortical neuronal mechanisms in flutter-vibration studied in unanesthetized monkeys: Neuronal periodicity and frequency discrimination.” In: *Journal of neurophysiology* (1969). 00592.

[9] Klas H. Pettersen & Gaute T. Einevoll. “Amplitude variability and extracellular low-pass filtering of neuronal spikes.” In: *Biophysical journal* 94.3 (2008). 00120, pp. 784–802.

[10] David Sterratt et al. *Principles of computational modelling in neuroscience*. 00081. 2011.